# Emerging robot swarm traffic

PENDERS, Jacques <http://orcid.org/0000-0002-6049-508X> and ALBOUL, Lyuba <http://orcid.org/0000-0001-9605-7228>

# Emerging Robot Swarm Traffic

Jacques Penders[1] and Lyuba Alboul[1]
[1]Materials and Engineering Research Institute
Sheffield Hallam University, Sheffield, UK
{j.penders, l.alboul}@shu.ac.uk

December 16, 2011

**Abstract**

We discuss traffic patterns generated by swarms of robots while commuting to and from a base station. The overall question is whether to explicitly organise the traffic or whether a certain regularity develops 'naturally'.

Human driven motorized traffic is rigidly structured in two lanes. However, army ants develop a three-lane pattern in their traffic, while human pedestrians generate a main trail and secondary trials in either direction.

Our robot swarm approach is bottom-up: designing individual agents we first investigate the mathematics of cases occurring when applying the artificial potential field method to three 'perfect' robots. We show that traffic lane pattern will not be disturbed by the internal system of forces. Next, we define models of sensor designs to account for the practical fact that robots (and ants) have limited visibility and compare the sensor models in groups of three robots. In the final step we define layouts of a highway: an unbounded open space, a trail with surpassable edges and a hard defined (walled) highway.

Having defined the preliminaries we run swarm simulations and look for emerging traffic patterns. Apparently, depending on the initial situation a variety of lane patterns occurs, however, high traffic densities do delay the emergence of traffic lanes considerably. Overall we conclude that regularities do emerge naturally and can be turned into an advantage to obtain efficient robot traffic.

*Keywords*:Swarm robotics; sensors and visibility; traffic patterns; traffic flow.

## 1 Introduction

In this paper we discuss the traffic generated by swarms of robots. The research is part of a larger project (Penders et al., 2011), which aims to operate a swarm of autonomous robots. The project's swarm approach is bottom-up (Crespi et al., 2008): we design individual agents and than look for the resulting or emerging group behaviour patterns.

Our robot swarm is designed to survey and inspect an industrial area, for instance a warehouse. The typical size of a warehouse is $(400 \times 100)m^2$, these dimensions certainly require a large number of robots. Our swarm consists of

homogeneous and autonomous robots; within the swarm the robots are anonymous, this means that the robots are able to recognise another robot as a robot but they cannot identify other robots as a particular individual with a unique name. The swarm will be able to operate in several autonomous modes. In the basic mode the robots navigate on their own and do not communicate, but just react to each other's behavior; it is a decentralised swarm (Kazadi, 2009). This non-communicative[1] mode of operation is the subject of this paper.

An additional communicative mode might complement the basic mode to allow 'higher' level cooperation, for instance coordinated navigation. However, the swarm is intended to be applied in a warehouse, the racks of which form a dense lattice of metal joints, moreover the racks might be packed with tins, cans or other metal based packagings. Thus, the reception of wireless signals is very variable and communication failures are to be expected. The non-communicative mode has to function as a fall back provision in case communication links fail. Moreover, this mode will also be applied to make the robots search for a (wireless) communication signal when connectivity is weak or is lost. The non-communicative mode is therefore essential to the robot swarm.

Our interest is in what we call *swarm traffic*: the robot traffic generated by a large swarm of homogenous robots. The robots are shuttling between a home or base station and their actual job, for instance to recharge their batteries. We call the traffic leaving the base station *outbound*, and the returning traffic *inbound*. As there will be quite some traffic up and down the central pathway, we call this the *highway*. We are particulary interested in how the robot traffic will develop on the highway. The aim is to obtain a reasonable throughput of the swarm traffic; the research question is whether we should organize the robot traffic explicitly or whether a certain regularity develops 'naturally'.

Obviously, on a chaotic highway the robots might loose much time avoiding each other and make little progress. The obvious paradigm of organized traffic is human driven motorized traffic, which is based on a rigid division of the road into a left and right zone, each with one-way traffic. In contrast to motorized traffic, human pedestrians find their way generally without any zonal distinction being imposed. In a crowded area, for instance a shopping center or an airport, human pedestrians generate a 'natural' or non-planned trail structure of a main trail in either direction and one or several secondary trails (Helbing et al., 2001). A remarkable 'in between' traffic pattern has been found with army ants. The ants follow a trail set out by their nest mates. Couzin and Franks (2003) report that during their overnight raids the main trail of the army-ants develops into a three-lane highway, in which the outbound ants utilize the outer lanes whilst the inbound ants travel on the inner lane.

The paradigm from the ants world is quite interesting. Ants have very limited brains, and are not supposed to be able to mentally overview the road and the traffic. The assumption is that they individually apply low-level behaviors that happen to lead to particular group behaviors of which the three-lane traffic pattern is an example. Our robot swarm is similar in that the robots also individually decide on their behavior, without having any overview. The point to investigate is whether group behaviors occur and whether our swarm

[1]Our robots do not leave signs or traces behind that could be picked up by fellow robots, therefore we do not use the term stigmergy, though some authors loosely define stigmergy so as to include our robots' behavior, refer for instance to (Beni, 2005).

of robots will develop certain traffic patterns. We start with using 'perfect' robots equipped with unlimited sensor systems and than, based on Couzin and Franks (2003) we implement ant inspired sensor models and a trail following mechanism to obtain robots that reflect certain ant characteristics. Thus we will also gain insight into whether our model captures the full mechanism that makes the army ants develop the three-lane pattern.

When studying emerging traffic, we assume that the highway is already defined: we are not concerned about how the trail was carved out. Thus, algorithms such as Ant Colony Optimization(ACO)(Dorigo and Stutzle, 2004) or Particle Swarm Optimization (PSO) are beyond our scope. Moreover, according to Beni, the study of these algorithms is not part of swarm robotics (Beni, 2005). To control the robot swarm, we apply the artificial potential force field method, which was introduced by Krogh (1984) and refined in Khatib (1986). Expositions of the method aiming at motion planning can be found in Latombe (1991) and Lee (2004). However, a robot swarm shows very dynamic behavior for which motion planning is not apt. In biological simulations often *self-propelled particle* (SPP) (Buhl et al., 2006) models are applied. Whereas the potential fields originate from field descriptions, the SPP models focus on describing the behavior of the individual agent, refer to the in biology often used (SPP) model of Vicsek et al. (1995). However, the details of swarm behavior are not yet fully understood, mainly due to the many parameters that may affect the behavior. Moreover, because of the complexity and the dynamics of the resulting behavior, swarm research usually restricts to generating outcomes of a general nature and aims at concepts such as 'formation control' (Gazi and Passino, 2004b) and 'clustering' (Kazadi et al., 2003) or 'gathering' (Flocchini et al., 2005) behavior.

To simplify the formal study of swarm control, one often assumes that each robot knows exactly the relative position of the other robots (Reif and Wang, 1999; Gazi and Passino, 2004a) and (Kazadi et al., 2003), we will say that in this case the robots have *perfect sensors*. In this paper we use this simplified context to explain the control model and we start with small groups for which we proof some group properties using constructive geometrical methods.

We drop the assumption of perfect sensors when studying the impact of variations in the sensor models. A robot observes its environment including the other robots with sensors. Based on this information each of the individual robots makes navigation decisions. The sensors and the design of the sensor system as a whole determine the type and quality of the information and therefore have a considerable impact on the swarm behavior. Flocchini et al. (2005) note that concerning variations and limitations of sensor systems, only few theoretically founded results are known and many interesting directions remain open. In our simulations each robot is treated as an individual agent with its own particular sensor system and decision making unit. We apply a variety of sensor systems, ranging from unrestricted perfect sensors to coarse and short ranged sensors.

The paper is organised as follows. In Section 2 we first discuss the control model, that is, the mathematical equations governing the robots and the swarm. We relate our model to the model of Reif and Wang (1999) and the more recent models of Gazi and Passino (2004a) and Gazi and Passino (2004b). For robots with 'perfect' sensors we proof two special situations observed by Penders et al. (1994). We use these situations in Section 3, where we introduce and evaluate the impact of limitations of the sensor systems in a group of three robots. Thus,

having set a background, we proceed with large groups and swarms. In Section 4 we define the highway and discuss simulations of robots traveling in strings. These simulations yield upper bounds for the expected traffic flow. In Section 5 we explore our main topic which is the generation of traffic patterns. We discuss traffic simulations in open space as well as in bounded space (i.e. a road). Moreover, we look at sparsely occupied and quiet roads as well as at an overcrowded highway.

# 2 The control model

The artificial potential field method is often used for controlling a robot swarm, refer to Gazi and Passino (2004b) for a modern description. As the name indicates, this method focuses on describing the potential field(s) in which the robots are to operate. Biological simulations often apply the self-propelled particle (SPP) models Vicsek et al. (1995). Similar to the model in Penders et al. (1994), the SPP models focus on describing the behavior of the individual agent; basically the two approaches are equivalent and can describe the same control models. The two approaches are some times referred to as Gaussian (integrative field based) and Lagrangian (individual based) (Parrish and Hamner, 1997). The advantage of the individual based SPP approach is that it is intuitive for empirical studies to observe individuals and build up a multiple agent system or swarm by adding individuals. In this paper we will follow the individual based approach.

Each robot $a$ calculates a force $\overrightarrow{F_a}$, which is the generator of the new velocity vector of the robot. In its general form the control model depends on four terms:

$$\overrightarrow{F}_a = \sum_{g \in G} \overrightarrow{EA}_{(g,a)} + \sum_{o \in O} \overrightarrow{ER}_{(o,a)} + \sum_{r \neq a}^{Sw} \overrightarrow{IA}_{(r,a)} + \sum_{r \neq a}^{Sw} \overrightarrow{IR}_{(r,a)} \qquad (1)$$

The first two terms represent the external influences; $\overrightarrow{EA}_{(g,a)}$ is the *attraction* of goal $g$ on robot $a$ and $\overrightarrow{ER}_{(o,a)}$ is the *repulsion* caused by the obstacle $o \in O$ on robot $a$. The second pair of terms in (1) consists of the internal forces, which originate amongst the robots in the swarm $Sw$. They are the attraction $\overrightarrow{IA}_{(r,a)}$ and repulsion $\overrightarrow{IR}_{(r,a)}$ between any swarm member $r$ and robot $a$. The attraction points directly towards the source object and the repulsion points into the opposite direction, away from its source. Obviously, if we consider $a$ to be a point and let it range over the two dimensional plane, each of the terms in (1) but also the terms together generate particular potential force fields, depending on the functions applied in the terms. Usually, the functions for attraction and repulsion are chosen such that on large distances the attractions $\overrightarrow{EA}$ and $\overrightarrow{IA}$ dominate while on short distances the repulsions $\overrightarrow{ER}$ and $\overrightarrow{IR}$ dominate. The internal attraction $\overrightarrow{IA}_{(r,a)}$ and internal repulsion $\overrightarrow{IR}_{(r,a)}$ are sometimes called the artificial social potential functions (Reif and Wang, 1999), as their combination induces coherence in the swarm. At a particular distance internal attraction and repulsion balance; this is called the *equilibrium distance* (Reif and Wang, 1999). Note that if only internal attraction applies but no repulsion, the robots will chase each other; if only repulsion applies the robots will disperse (Penders et al., 1994).

To introduce our simulation model, we first specify the internal force system. We also fix a *linear unit of distance*, to which we refer simply as a *unit*. Swarm cohesion is not sought for in our application, thus we set the internal attraction $\overrightarrow{IA}$ to zero. Contrary to Reif and Wang (1999), our swarm consists of anonymous robots and the robots react the same to any other robot thus the magnitude of the internal repulsion depends only on the distances between the robots:

$$\|\overrightarrow{IR}_{(ab)}\| = 1/\mathrm{dist}(a,b)^2; \text{ with } \mathrm{dist}(a,b) \text{ being the Euclidean distance.} \quad (2)$$

The robots are homogeneous, thus:

$$\overrightarrow{IR}_{(ab)} + \overrightarrow{IR}_{(ba)} = \overrightarrow{0};\ a,b \in Sw \quad (3)$$

The function applied in equation (2) does influence the detailed behaviour of the swarm of robots, however our main results discussed below apply on any function as long as the function is differentiable and the same for each robot. Equation (3) however is crucial in our proofs below. We define the external repulsion of objects $\overrightarrow{ER}_{(o,a)}$ for $o \in O$, $a \in Sw$ similar to the internal repulsion, but since we want objects to have only a local influence, we restrict the range of their influence:

$$\begin{aligned} \|\overrightarrow{ER}_{(o,a)}\| &= 1/\mathrm{dist}(o,a)^2, \text{ if } \mathrm{dist}(o,a) <= 3, \\ &= 0, \text{ elsewhere.} \end{aligned} \quad (4)$$

For the external attraction $\sum \overrightarrow{EA}_{(g,a)}$ equation (1) allows many variants. In this paper the magnitude of the attraction is the same for all robots at every point of the plane (we discuss some variations in section 5) :

$$\|\sum_{g\in G} \overrightarrow{EA}_{(g,r)}\| = \|\sum_{g\in G} \overrightarrow{EA}_{(g,s)}\| = 0.5\times maxspeed = \text{constant; for all } p \in \mathbb{R}^2; r,s \in Sw. \quad (5)$$

Within this constraint we consider three different cases; the basic cases are: (i) each robot has one single goal and the direction of the attraction varies with the position of the robot relative to the goal; (ii) each robot has a fixed travel direction meaning that the direction and the magnitude of the attraction are fixed and the same for all points in the plane; the third case (iii) applies for trail following robots, on the trail the attraction has a fixed direction as in (ii) while off the trail the attraction points back to the trail. Case (iii) is a multiple application of (ii) in that directions vary for different sections of the plane, we discus this in more detail below in Section 3. Though we apply only these relatively simple cases other variants may, for instance, include: a set of multiple goals, or models in which the external attraction is determined by a non-constant function assigning values to the points of the plane refer to Gazi and Passino (2004a,b). When, as mentioned in the introduction, our swarm is to search for a wireless communication signal the attraction is determined by the signal strength and the function representing this strength will not be trivial.

The distinction between the internal and external attraction and repulsion is essential for understanding the behavior of the swarm. A force system may have invariant points, invariant points depend on the functions applied and may differ considerably. As Penders et al. (1994) and Gazi and Passino (2004a) show,

the distance dependent internal forces defined by equation (2) above have the centroid of the swarm as an invariant point. In other approaches, for instance Baldassare et al. (2002), the centroid is used as the main reference point for formation control. However, often robots are not capable of distinguishing between obstacles and other robots, whereby the distinction between internal and external repulsion is blurred, and the robots only perform collision avoidance (Khatib, 1986).

As said at the beginning of this section the force $\overrightarrow{F_a}$ resulting from equation (1) is the basis for generating the new velocity vector of the robot. Reif and Wang (1999) note that there are many ways to transfer the force $\overrightarrow{F_a}$ into a movement/displacement of the robot. In our simulations, if the force sum at time point $t$ is $\overrightarrow{F_{(a,t)}}$ and robot $a$ is at position $x_{(a,t)}$ the displacement is calculated as:

$$x_{(a,t+1)} = x_{(a,t)} + (\overrightarrow{F_{(a,t)}}/\|\overrightarrow{F_{(a,t)}}\|) * min(\|\overrightarrow{F_{(a,t)}}\|, maxspeed). \tag{6}$$

Equation (6) does not account for the dynamics of a real robot. Gazi (2005) therefore calls such models *kinematic models* for swarm behavior. As in our studies, they are aimed to be used for proof of concept studies. Introducing the full dynamic behavior of a real robot into a simulation brings a heavy computational load with it, an approximation is proposed in Gazi (2005). Similar to our approach in equation 6, simulations of biological system usually do not account for the dynamics of bodies, refer to Vicsek et al. (1995). In their ant traffic simulations Couzin and Franks constraint the movements of ants by applying an empirically determined maximum turning rate and maximum acceleration (Couzin and Franks, 2003).

## 2.1 Basic cases

Three robot systems are analysed in Penders et al. (1994) and Penders et al. (2004). The analysis is based on a simplification of (1) in which internal attraction $\overrightarrow{IA}$ is absent and each robot has only a single goal $G$, refer to (7); the attraction of the goal is defined as in equation (5). The papers investigate cases where external attraction $\overrightarrow{EA}$ and internal repulsion $\overrightarrow{IR}$ either are in or close to an equilibrium. We recall these cases as they illustrate some of the aforementioned statements and they also provide a good basis to evaluate sensor models.

$$\overrightarrow{F}_a = \overrightarrow{EA}_{(G,a)} + \sum_{r \neq a}^{Sw} \overrightarrow{IR}_{(r,a)} \tag{7}$$

*The internal force system.* Typically for the system of internal forces:

*Observation* 2.1. The centroid of the robots (*CentR*) is an invariant point ((Penders et al., 2004),(Gazi and Passino, 2004a)).

*Observation* 2.2. If the group of robots are not on the same line, then the internal repulsive forces make the robots move towards a position in an equilateral triangle, while the centroid *CentR* does not move (Penders et al., 2004).

In Alboul et al. (2008) observation 2.2 is extended to larger groups and shows that one or more equilateral polygon(s) are formed.

*The external force system.* Forced by the external attraction the whole robot team moves, meaning that the centroid *CentR* moves. The system of external forces may also have invariant points. Provided that the goals are in a general position and form a general triangle (angles $< 120°$) and none of the goals $G_a$, $G_b$ and $G_c$ coincide or are on the same line Penders et al. (2004) prove:

*Observation* 2.3. At the Steiner point of the triangle of goals, the sum of attractions $\sum_r^{Sw} \overrightarrow{EA}_{(G,a)} = \overrightarrow{0}$ and the Steiner point is the unique invariant point for the attraction.

To study the dynamics of a robot team, the points of particular interest are those where an equilibrium occurs between the internal and external system, usually because the repulsive and attractive forces cancel out against each other. A simple example for a two robot systems is shown in figure 1. In the upper part two robots have a head-on encounter and at a certain point the attraction equals the repulsion causing the robot to come to a stand still, defined as a 'Balanced conflict' in (Penders et al., 2004).

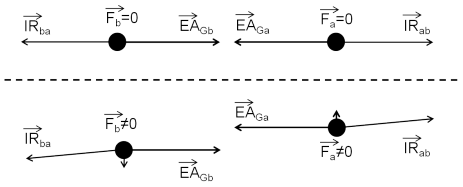


Figure 1: Upper part, a two robot encounter on one line, the repulsion cancels out the attraction; Lower part, slightly off the line small side way forces result; figure is not scaled.

The case for a three robot team is analysed in (Penders et al., 2004), it shows that in a balanced conflict the three robots form an equilateral triangle while the centroid *CentR* coincides with the Steiner point of the goals and moreover the *CentR* is on the base lines through $[G_{r_i}, r]$, for all robots. This type of balanced conflict is a particular case of a larger class of turning conflicts. Figure 1, lower part shows an example of two robots that will turn aside to pass each other. Below we recall from Penders et al. (2004) the case for three robots. We note that the case can be generalized to teams of $n$ robots and $n$ goals.

**Lemma 2.1.** *(**Turning Conflicts of 3 robots**) A conflict, in which the goals and the robots form equilateral triangles and the centroid CentR coincides with the Steiner point of the goals, but in which the robots are not situated on the base lines $[G_{r_i}, Steinerpoint]$, is not a balanced conflict, moreover while the conflict is evolving, the robot-team will turn.*

Figure 6 shows an example of lemma (2.1), we use the case below to evaluate the impact of the sensor model. Note that the balanced and turning conflicts require that the robots are inside the triangle (hull) formed by the goals. For the traffic simulations we also apply equation (5) but define a fixed travel direction for the robots (above discussed as case (ii)); thus in the traffic simulations the robots are relatively close but the goals are far away on one side of the robot team.

**Lemma 2.2.** *(**Far-Away Goals**) Assume that the goals of the robots are infinitely far away, though all situated in the same direction. Moreover, assume that two robots (a and c) are on a line orthogonal to the direction of the goals, and the third robot (b) is between the course of the robots (a and c) to their goals, (refer to figure 2) then three cases are possible:*

1. *Case a: if all three robots are on the same line l (as shown in figure 2), they proceed towards the goals while remaining on a line parallel to the initial one.*
2. *Case b: assume that robot b is a little behind, then b will always remain behind the line connecting a and c.*
3. *Case c: assume that robot b is ahead, then b will always remain ahead of the line connecting a and c.*

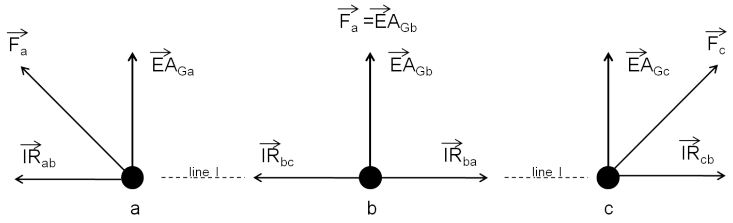


Figure 2: Three robots on one line, goals infinitely far away; the forces are sketched (not scaled).

**Proof case a.** Easily understandable from figure 2. All repulsive forces work in directions parallel to the line formed by the robots, and have no component in the directions of the attractive forces. Remark, robot $b$ will tend to a position just in the middle between $a$ and $c$, so that $\overrightarrow{IR}_{(b,a)}$ equals $\overrightarrow{IR}_{(b,c)}$.

The proofs for cases b and c are similar.

**Proof case b**. The repulsive forces $\overrightarrow{IR}_{(b,a)}$ and $\overrightarrow{IR}_{(b,c)}$ have a non-zero component, pointing into the direction opposite of $\overrightarrow{EA}_{(b)}$, whereas $\overrightarrow{IR}_{(a,b)}$ and $\overrightarrow{IR}_{(c,b)}$ have a component adding positively to $\overrightarrow{EA}_{(a)}$ and $\overrightarrow{EA}_{(c)}$.

**Proof case c.** The repulsive forces $\overrightarrow{IR}_{(b,a)}$ and $\overrightarrow{IR}_{(b,c)}$ and have a non-zero component adding positively to $\overrightarrow{EA}_{(b)}$, whereas $\overrightarrow{IR}_{(a,b)}$ and $\overrightarrow{IR}_{(c,b)}$ have a component pointing into the direction opposite to $\overrightarrow{EA}_{(a)}$ and $\overrightarrow{EA}_{(c)}$. This ends the proof of Lemma 2.2.

**Corollary 2.3.** *Under the conditions of Lemma 2.2 case a, the robots disperse along a line parallel to the line l.*

**Proof** Straightforward from the proof of case *a*.

In the traffic simulations we will also have robots with goals in opposite directions (inbound versus outbound robots) as shown in figure 3, where robot $b$ encounters robots $a$ and $c$. If robot $b$ is on the bisector of $a$ and $c$ it will slow down, but not deviate from its course, as is clear from the forces working on robot $b$. Robots $a$ and $c$ will turn aside to the left and right respectively. If robot

$b$ is not on the bisector but also not encountering any of the other two head-on, that is on the base line of the attractive forces, robot $b$ will tend towards the bisection. Argumentation as in case $a$ above.

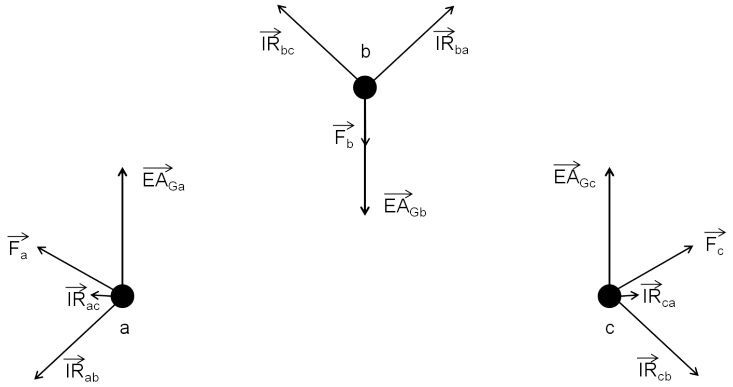


Figure 3: Two robots on a line orthogonal to the direction of their goals, encountering a third robot traveling in the opposite direction

Furthermore, the traffic simulations will deal with two groups of robot, again with the directions of the goals parallel but opposite. One row of inbound robots may encounter a row of outbound robots, refer to figure 4. Combining the above insights for this situation we can predict the following. If the rows are infinitely long and evenly spaced and the robots are positioned on the bisectors between individuals of the other group, each row will slow down but they will not adapt their respective courses. If the opposite group is not strictly on the bisector but also no individual is encountering any of the opponents head-on on the base line of the attractive forces, each individual will tend towards the bisection of its direct opponents.

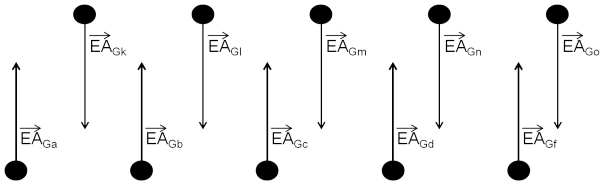


Figure 4: Two rows of opposed robots

In the sections below we will be looking for lane patterns in the traffic of the robot swarms. The mathematical considerations of the current section indicate some important issues in advance of that discussion. The major suggestion is that if no head-on encounters occur between the opposed groups of (inbound and outbound) robots, any existing lane pattern will be preserved.

# 3 Sensors

The control model (1) is often applied such that all robots have perfect knowledge about the whereabouts of all other robots (refer to Gazi and Passino

(2004a) and its references); such robots have *perfect sensors*. However, real sensor systems are usually limited, and their limitations reflect on the behavior of the robots and the swarm.

Below we discuss swarms of robots with *limited visibility*; i.e. each robot observes its surroundings no further than a fixed range or distance $\rho_{max}$. With regard to the control model, the restricted visibility results mathematically speaking into partitioning the space into bounded regions, which brings our model closer to the models arisen in discrete mechanics (Baez and Gilliam, 1994).

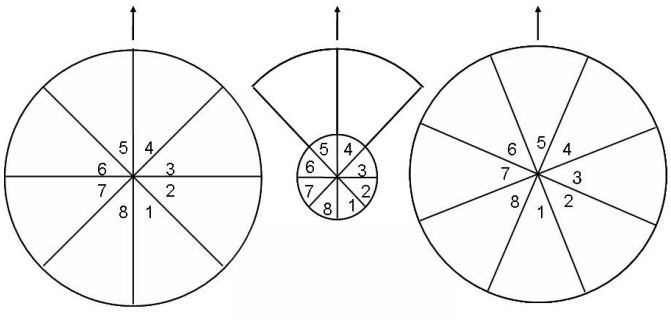


Figure 5: Standard 8 sector sensor (left); Ant-sensor (middle); Shifted (right); not to scale.

Our robots are equipped with sector sensors; these are sensors that scan the environment in circle sectors, equally spread anti-clockwise over the 360° field, refer to figure 5 (left most drawing). Though the number of sectors is variable, in most simulations eight sectors are applied such that each covers $\pi/4$ or 45°. The front and backsides of the robots are fixed. The first sensor sector starts at the back of the robot from the line through the center of the robot. When an object is spotted in a sector, only the closest distance is measured and used to calculate the repulsive force (equation (2)) with an orientation along the bisection of the sector. In reality (and in our simulations) robots have an extension, thus the sensors might spot another robot in more than one sector. We also note that because of the limited and coarse sensors, situations as described in lemma 2.2 apply in swarms of any size. If $n$ robots are close to be on one line cases $a$ to $c$ may apply to each triple of neigbouring robots. However, the conditions to these cases do not concern the exact positions of the robots but their representation by the sensor system of the other (observing) robots. The sector design also results in a particular discrete representation of a wall. For each sector, the sensor system computes only the distance to the nearest point of the corresponding parts of the wall, and represents that part of the wall by the distance along the bisection of the sector. Therefore, our robots 'perceive' the wall as a finite number of discrete objects (wall sections), and not as a continuous object. Note that a suitable set of point obstacles may generate the same representation.

The sensors have a range limit usually set to 15 *units*, beyond which nothing is observed. Robots equipped with the eight sector sensors and with all sensor sectors set at the same limit, are for convenience referred to as **standard robots**. However, the range of the sensor may be varied per sector, allowing to define what we call **ant sensors** which model the senses of ants following the

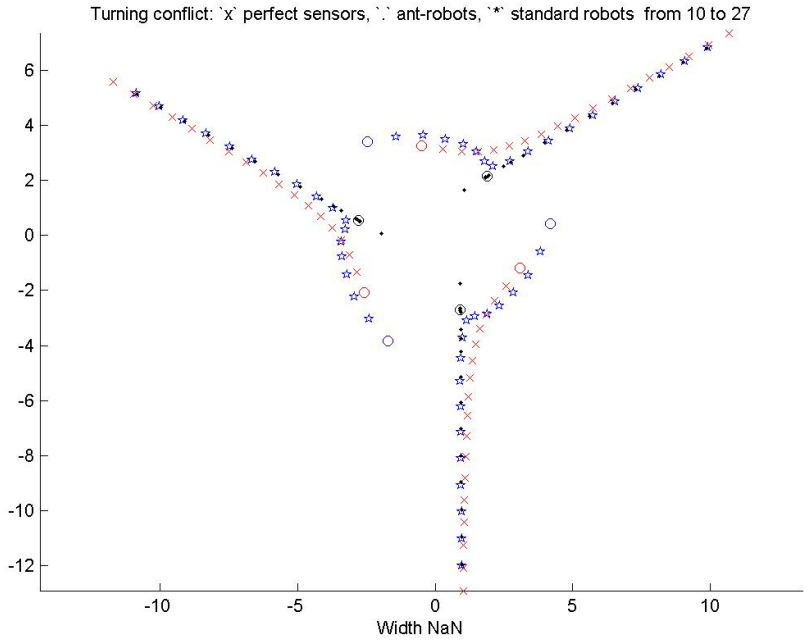


Figure 6: Turning conflict of robots with ant-sensors, standard robots, and robots with perfect sensors. Open circles represent the current positions of the robots; the full trail for each type of robot is shown.

description in Couzin and Franks (2003). Referring to figure 5 (drawing in the middle) the front two sectors (numbers 4 and 5) are retained at the full range (of 15 *units*) while the ranges of all others is reduced to 3 *units* only. The two front sectors represent the area covered by the antennae of an ant. The close range sectors cover the body and the legs of the ants. We deviate from the model of Couzin and Franks (2003) only in that the ratio between the larger and the close range sectors is 5; in the original model the ratio is just 2. The close range sectors should not be omitted: without them two robots may move side by side at close distance without noticing each other, and any small sideways reaction would make them collide.

We try the sensor models with groups of three robots situated in a turning conflict, as described in lemma (2.1). The first group consists of robots with perfect sensors, for this group the mathematics of the previous section applies straightforwardly. The second group are standard robots, and the third consists of robots with ant sensors. The simulations are shown in figure 6. The typical difference in the behavior of these groups is that the robots with perfect sensors show smooth courses, whereas the standard robots show abrupt changes. The abruptness is due to the fact that the sensor system introduces coarseness: it represents any object as if positioned on the bisection of the sector. The robots form an equilateral triangle, however their courses are not on the baselines $[G_r, EPG]$ (it is a turning conflict). Thus when getting close enough,

the robot on their left side appears suddenly in a second sensor sector inducing considerable repulsion. The ant sensor has only two sector and this effect will not occur, these robots end up in a balanced conflict (refer to the trails of dots in figure 6, note that the current positions (open circles) are on the straight lines formed by the trails).

# 4 The Highway

We are to explore the generation of traffic patterns on a highway, where all robots are given a fixed traveling direction. We deal with two groups traveling in parallel but opposite direction, representing a group of inbound and a group of outbound robots, also referred to as north-bound and south-bound[2].

In (Couzin and Franks, 2003) army ants are described, basically the ants do follow a trail. In order to model ants we implement also trail following. Thus we can define our *ant robots* as robots that have ant sensors and that apply trail following. However, as corollary 2.3 and the discussion following it states, in open space the internal repulsion will cause our standard robots to disperse, refer also to Penders et al. (1994); figure 7 shows a simulation[3]. To be able to observe the behaviour of standard robots on the same space as the ant robots we define a bounded highway. Having defined a highway we explore the characteristics of robot traffic in predefined lanes. Obviously there will be quite some similarities with human driven motorised traffic. Since we are dealing with robots we can manipulate the traffic in detail, thus we obtain criteria to evaluate the swarm traffic in the next section.

## 4.1 Trail and trail following

Natural ants follow a trail of pheromone, created as the ants deposit pheromone while travelling. Newly arriving ants follow trails carved out by some explorer and also deposit pheromone. The concentration of pheromone increases with ants passing, but it also diffuses. Trail forming is extensively studied in Ant Colony optimisation (refer to Dorigo and Stutzle (2004)); however we are considering an established trail. Couzin and Franks (2003) note that for an intensely used trail one can fix the pheromone concentration. Thus we simplify and define a uniform trail stretching from north to south, the width of the trail is adjustable.

The robots are provided with a trail following mechanism; when the robots are on the trail the direction of their goal is fixed to either north or south. Off the trail, goal finding is adjusted to make the robots search for the trail. We have imitated the policy of a natural ant. Ants have two antennae with which they track the pheromone trail. When one of the antennae receives stronger input (that is when it is closer to the trail) the ant turns into that direction to get back to the trail (Couzin and Franks, 2003). Our trail robots behave similarly, when off the trail they turn over an angle of ($1/4\pi$ max) towards the trail. If the robot's orientation is orthogonal to the trail a random direction is selected, again similar to a real ant (Couzin and Franks, 2003). Thus, off the trail the north/southbound aspect is ignored; the result is that in the simulations when

[2]Full details of the simulations are given in section (4.3) below.

[3]From figure 7 onwards all figures have the same format, refer to section 4.3.

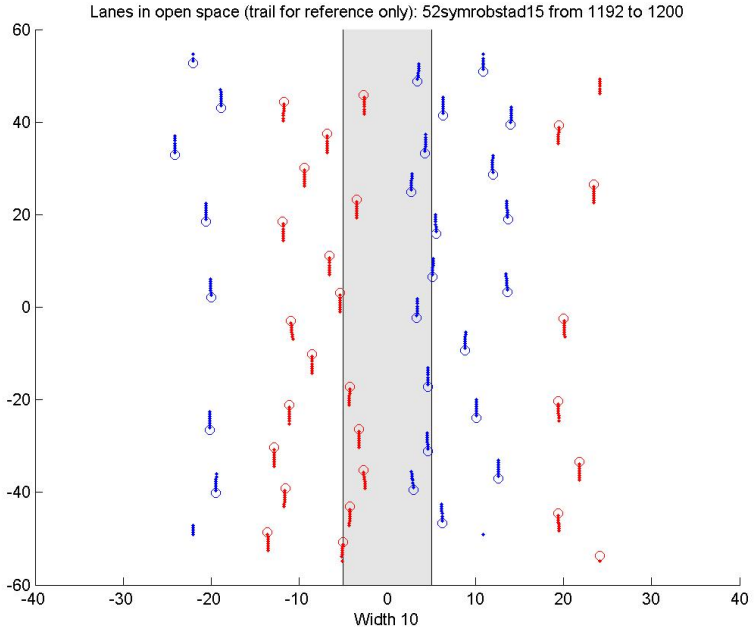


Figure 7: Standard robots in open space with a trail drawn for reference only. Simulation results in table 2, row 1.

off the trail the trail robots often display circular courses. Defining a trail and implementing trail following allows for a 'softly' defined highway.

## 4.2 Hard defined highway

We define a rigid highway layout by applying two outer walls to obtain a two way road and if one-way lanes are required we add a third wall in the middle. The two way road has a width of 16 *units*; the one-way lanes - figure 9 shows the layout - have a width of 8 *units*. The robots are sensitive to static obstacles only within a range of 3 *units* (equation 5), thus on the one way road there remains a passage (2 *units* wide) where the robots are not subject to repulsion from the walls.

## 4.3 Simulation details.

Below we discuss simulations with swarms of robots on the highway. We compare the behavior of robots with full sector sensors as well as robots with ant-sensors. Moreover the robots may apply trail-following. Therefore we have basically three main types of robots:

1. *Standard robots* subdivided into
   (a) Standard robots with the 8 sector sensors (figure 5, left)
   (b) Standard robots with shifted 8 sector sensors (figure 5, right)

2. *Trail robots* which apply trail-following, they are equipped either with
   (a) the 8 sector sensors (figure 5, left) or
   (b) with shifted 8 sector sensors (figure 5, right)
3. *Ant robots* equipped with ant-sensors (figure 5, middle) and applying trail-following.

The highway, whether defined by walls or consisting of a trail, stretches from $y = -60$ to $y = +60$. For convenience, we refer to the groups of robots as north-bound and south-bound; north is towards the top of the screen $y = +60$ and south downwards $y = -60$. When a robot arrives at the far end (surpassing $y = \pm 50$) of the highway it is swapped back to the other end to simulate on-going traffic, also in order to propagate the developing traffic pattern the horizontal-position of the robot is retained in the swap operation, for instance a robot ending at $(0, 50)$ is swapped to $(0, -50)$. However, to avoid projecting robots on top of each other some variation had to be introduced in their new $y$ positions (this affects the speed calculations slightly). In the simulations the robots are given a circular extension of radius 0.25 *units*.

In the simulations $maxspeed = 1$ *unit/tick*, thus a cruising speed of 0.5 *units/tick* results from equations 5, 6 and 7 if there is no repulsion. All our simulations are based on a discrete time model. Given the position of the robots at a time point $t - 1$, the situation at time point $t$ is generated by letting each robot observe $t - 1$ and calculate a course up to time point $t$, as prescribed in equation (6). The conjunction of all these steps constitutes the situation at time point $t$. Thus our simulations show time slices of what can be considered a continuous evolution of our swarm, resulting in models similar to discrete dynamic systems. The discrete model of time is a source of abruptness as each robot makes a full step at a clock tick. To avoid that a robot may jump onto (or over) another robot, we introduce a safety zone $sz = maxspeed + 2 \times extension = 1 + (2 \times 0.25) = 1.5$ *units* around the robot. Thus the repulsion -refer to equation (2)- is implemented as:

$$\|\vec{R}_{ab}\| = 1/(dist(a, b) - sz)^2. \tag{8}$$

Note that the sensors and the control model are implemented without any randomiser. The simulations with the standard robots are therefore fully deterministic. In the trail following procedure a single random factor occurs when a robot is off the trail and faces a direction perpendicular to the trail (refer to the trial following procedure discussed above). However such occasions occur rather seldom and in practice most of the simulations involving trail following are deterministic as well and quite reproducible.

#### 4.3.1 Swarm size and figure and table conventions

**Swarm size.** The simulations effectively use an area of 100 *units* length and a variable but fixed width, the swarm size therefore characterises traffic density. As explained below, the traffic strings can run at any density up to $2 \times 66$, as long as the safety zones ($sz = 1.5$) are not infringed. We apply $2 \times 23$ robots spaced at 4 *units*. For the swarm traffic we run for each type of robot simulations with swarms of various sizes. In the dense swarms of 52 robots the average distance

between the robots is 3.7 *units*. The repulsion between robots equals the (0.5) attraction of the goal at a distance of 2.9 *units* (equation 8). In the rather loose swarms of 26 the average distance is 5.2 *units* resulting in a relatively weak mutual repulsion of 0.07. To provide a feel of what happens between 26 and 52, we apply also swarms of intermediate sizes with 42, 37 and 22 robots. The initial situations are described below in subsection 4.3.2.

**Figures.** Starting from figure 7 onwards all figures showing robot swarm simulations follow the following conventions: the current position of each robot is shown by a small open circle and the previous 8 positions are given as (a tail of) dots. The titles above the plots, provide a short characterisation, for example in figure 7 : 'Open space...'; the name of the parameter file: '52robstad15'; and the time points displayed, from clock tick '1192' to clock tick '1200'. 'Width' at the bottom indicates the width of the trail.

**Tables.** Not all simulations result in perfect lane traffic. In some simulations huge jams occured which did not resolve in the duration of our simulations, the tables indicate this by 'jam': figure 14 shows an example. Typically some individual robots do escape from the jams but at the same time new robots get stuck. Even at clock tick 7200 the jam of figure 14 had not dissolved. To project this to a human environment: our robots have a cruising speed of $0.5 units/clocktick$; $1 m/sec$ is a reasonable speed for a pedestrian; so 7200 clock ticks would resemble a 1 hour delay for human pedestrians.

As lemma 2.2 shows and the figures indicate, if no head-on encounters occur the lane pattern will not change and is *stable*. In the tables the indication 'ns' stands for *Non-Stable* and means that a full division into lanes or zones has not occurred yet and both groups still have head-on encounters with members of the other group, refer to figure 8. Lane numbers with the addition 'ns', for instance '3 ns', indicate that distinctive lanes have developed but a few robots (one or two) have not carved out a proper lane and continue having head-on encounters.

### 4.3.2 Initial situations.

The positions from which the robots in the swarm start have a significant influence on the behavior of the swarm. Section 2.1 indicated that if no head-on encounters occur between the opposed groups of (inbound and outbound) robots, any existing lane pattern will be preserved. Also the string simulations show that the strings might slightly deform, but the subdivision into two traffic zones is preserved throughout the simulations; the simulations of table 1 rows 14-18 are allowed unlimited space, nevertheless all have the space divided into two zones. This is no surprise: on a lane or zone the attraction is the dominant force working either in the north or south direction (direction of the $y$-axis). While in the east-west ($x$-axis) direction the traffic strings from the other group generate a repulsive barrier. In order to investigate the influence of the initial situation, we arrange several different situations in which the north and south bound robots are uniformly mixed. They are placed within an area 10 *units* wide, and the robots initially face directions unrelated to their destination with for each group the sum of the orientation angles equal or close to a multiple of $2\pi$. Three initial situations and the first 10 clock ticks are shown in figure 8. The first clock tick is not part of the simulation but serves to give the robots an initial direction; the situation at the second clock tick is the actual initial

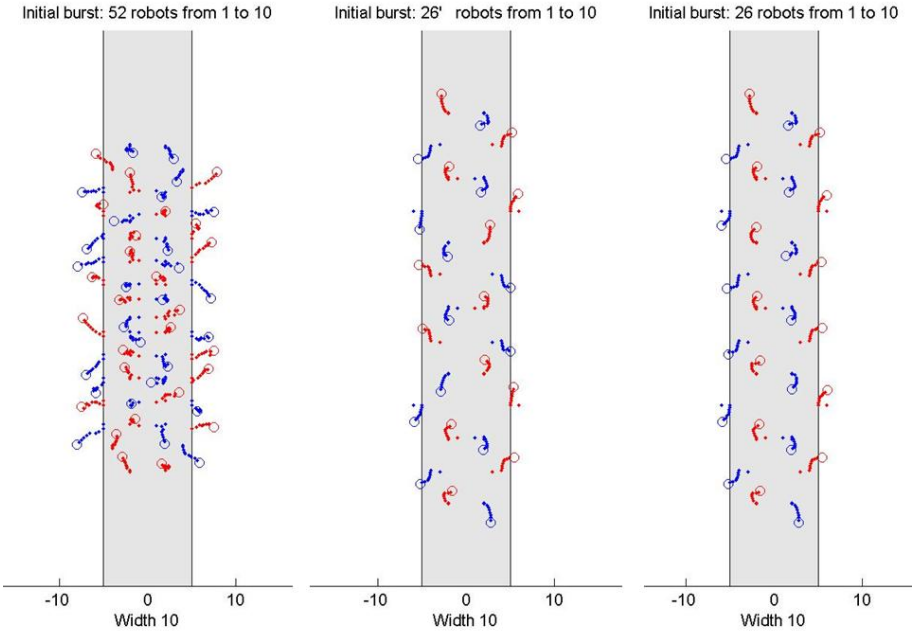


Figure 8: The first 10 clock ticks of swarms of 52 (left) and 26 (middle and right) robots; the right most swarm of 26 is pre-arranged into (none straight) lanes.

situation.

The initial situation for the 52 robot swarm is shown on the left in figure 8. The robots are positioned such that in the horizontal direction $\sum x_{north} = \sum x_{south} = 0$; while vertically $\sum y_{south} = -\sum y_{north} = 70$ both groups have two robots extra at $x = 35$ for the south bounded and $x = -35$ for the north bounded group. The situation is also composed such that each vertical line of robots contains always both north and south bound robots, thus ensuring many head-on encounters. As the figure shows this dense swarm initially bursts out due to the repulsion amongst the robots, and at clock tick 10 only a few robots are heading into the proper direction, quite distinct from the 26 robot swarms shown in the middle and on the right in figure 8. The 26 swarm on the right hand side is positioned such that in the horizontal direction $\sum x_{south} = -\sum x_{north} = 15$ and vertically $\sum y_{south} = \sum y_{north} = 0$; the initial situation includes four lanes, two for each group. For the $26'$ swarm in the middle, the ten robots in the middle have swaped groups resulting into: $\sum x_{south} = -\sum x_{north} = 9$ and $\sum y_{south} = \sum y_{north} = 0$. By breaking up the initial lanes we force head-on encounters to occur.

The initial situation of 42 robot swarms is derived from the situation for 52 robots by deleting 10 robots around $y = 0$, resulting into: $\sum x_{north} = \sum x_{south} = 10$; while vertically $\sum y_{south} = -\sum y_{north} = 2$. In addition, we use swarms of 22 and 37 robots, their initial situations are roughly uniform but slightly asymmetric.

## 4.4 Traffic strings

Before discussing emerging traffic patterns, we have a look at organised traffic as this might deliver an upper bound for review and evaluation. In motorized traffic, strings of cars are a feature of busy motor ways, and under the proper conditions strings yield the highest throughput (Darbha and K.R., 1999), a fact that is also true for pedestrian traffic (Young, 1999). Thus, *string stability* is a wanted feature, in a stable string the spacing between vehicles remains nearly the same (Darbha and K.R., 1999). However, car drivers are influenced by many factors and vary their speed (and mutual distances) accordingly. In contrast, the robots are homogeneous and behave identical in the same situation: all apply the same control model and have the same maximum speed.

From the control model (1) it is clear that the behavior of the robots depends mainly on their sensor system. Robots with perfect sensors in a string will be sensitive to all robots to the front as well as those to their back. In a finite string, the robots at the front of the string are subject to repulsion from the many robots behind them and will speed up, the reverse is true for the ones at the rear, they slow down or even might move backwards. Consequently, robots with perfect sensors will neither form nor preserve a stable and equally spaced string. Only when the string is infinitely long to both ends, it will be equally spaced. Moreover, if no maximum speed is applied, the string might travel at arbitrarily high speed, this is a problem noted for motor traffic simulations (Darbha and K.R., 1999).

Our robots are restricted by a maximum speed and also their sensors are limited. The standard robots are sensitive to what is happening in front as well as behind them. However they are sensitive only to the nearest robot. Thus when placed in an equally spaced string with $front$ being the nearest robot in

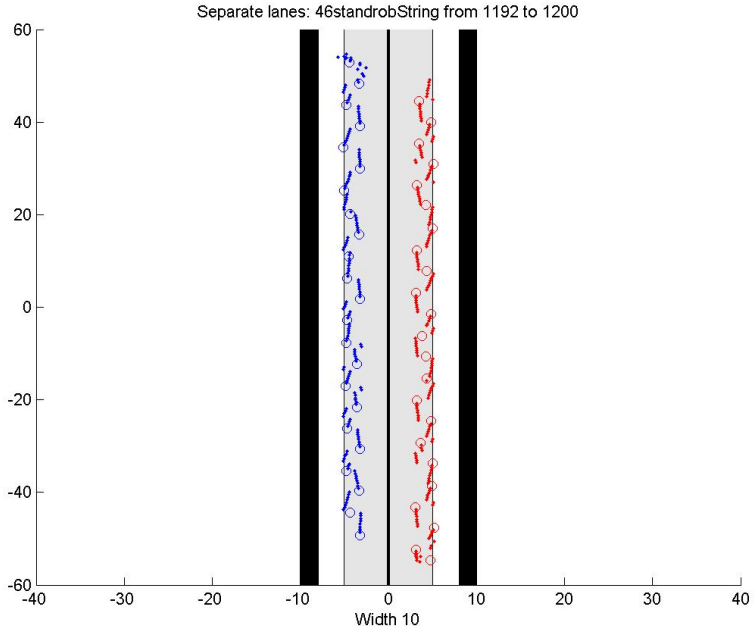


Figure 9: Strings of standard robots on two one-way lanes, trail drawn for reference only. Note the zigzag pattern. Simulation results in table 1, row 1.

front and *back* the nearest at the back we have for all robots $r$ except the first and the last one: $\overrightarrow{IR}_{(front,r)} + \overrightarrow{IR}_{(back,r)} = 0$. As a result, within a string only the external attraction ($\overrightarrow{EA}$) is effective, which is constant and the same for all robots. Thus we may expect to generate a nearly stable string moving at a constant speed equaling the cruising speed of 0.5 *units/tick*. The cruising speed results from equations 5, 6 and 7 if there is no repulsion. However, as figure 5 shows, the edges between sensor sectors 4 and 5, and 1 and 8 coincide with the orientation of the string of robots. When running simulations, small rounding errors cause disruption of the strings and the robots will form a zigzag string, refer to figure 9. This can be compensated for by shifting the sectors over an angle of $1/8\pi$ as shown in the right most drawing in figure 5; thus sector 5 becomes the front facing and sector 1 the rear facing sector. When in a string, these robots remain in a nearly straight line, refer to figure 10. The ant-sensors do not allow the sensor shift; as a consequence the ant robots always tend to a zigzag string.

### 4.4.1 String simulations.

The string simulations start from an initial situation in which each group of robots is lined up at ($x = -4$) for the northbound and ($x = 4$) for the southbound group, mutual spacing within the groups is 4 *units*. The trail robots and the ant robots by definition do not require the outer walls to remain on the trail. It is nevertheless interesting to evaluate their behavior when the two groups are

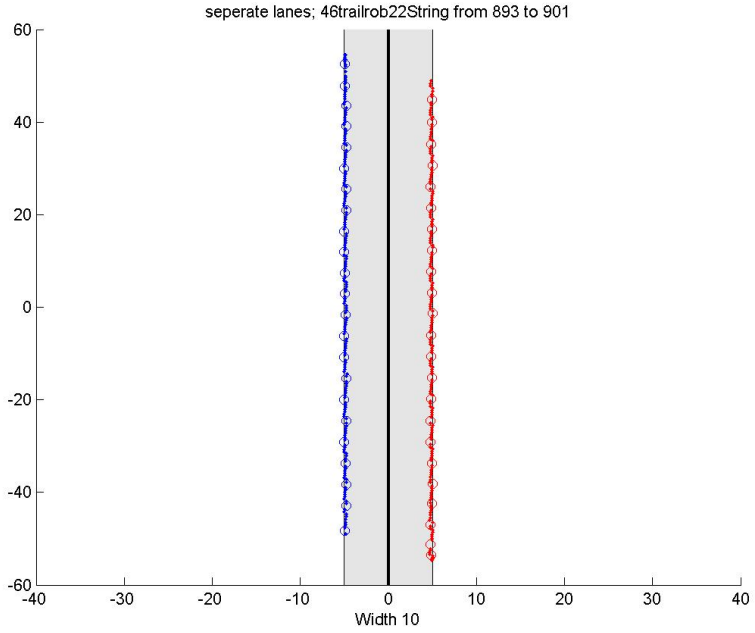


Figure 10: Strings of trail robots with shifted sensors on two one-way lanes. Simulation results in table 1, row 7.

separated by a wall in the middle. For comparison all possible configurations are tried: the one way lane structures with three walls and one wall as well as the two way lanes marked of by two outer walls and open space. Table 1 shows the resulting average speed of the robots in the string simulations. In the first block of simulations (rows 1-5) the layout of the highway is as in figure 9, in the second block (rows 6-8) the layout is as in figure 10, the third block's (rows 9-13) layout is that of figure 13 and the last block of simulations (row 14-18) uses open space, refer to figure 7. Most patterns settle before 600 clock ticks, therefore the average speed between 600 and 1200 is given separately. The simulations involve 46 robots and their cruising speed is 0.5 *units/tick*. The standard robots' speed of 0.496 is close (99%) to the cruising speed (refer to row 1 in table 1) a little bit of the speed is lost as the robots incidentally get too close to the walls (refer to figure 9). The swarms of robots with shifted sensors loose some speed as the last robot at either end is for a period (until the next robot is placed behind) susceptible to repulsion only (refer to figure 10). Nevertheless, these robots are considerably faster than the ant robots, the latter travel at only 0.395 (or 79% of the cruising speed) in the best configuration (row 13 in table 1). The reason is that the ant robots do not observe the robot behind themselves (refer to the difference in sensor ranges shown in figure 5 middle), thus while the external attraction $\overrightarrow{EA}$ is constant, the repulsion $\overrightarrow{IR}_{(front,a)}$ reduces their speed.

| | *Average speed up to clock tick* / *Type of robot* | *150* | *300* | *600* | *1200* | Speed, 600 to 1200 |
|---|---|---|---|---|---|---|
| **Strings in two one-way lanes marked off with walls** | | | | | | |
| 1 | standard robots | **0.490** | **0.494** | **0.495** | **0.496** | **0.497** |
| 2 | standard robots sensors shifted | **0.467** | **0.470** | **0.471** | **0.472** | **0.473** |
| 3 | trail robots | **0.477** | **0.481** | **0.482** | **0.484** | **0.486** |
| 4 | trail robots sensor shifted | **0.463** | **0.466** | **0.468** | **0.469** | **0.470** |
| 5 | ant-robots | **0.343** | **0.354** | **0.361** | **0.364** | **0.366** |
| **String in two separate lanes, no outer marking** | | | | | | |
| 6 | trail robots | **0.463** | **0.463** | **0.460** | **0.459** | **0.458** |
| 7 | trail robot sensors shifted | **0.462** | **0.462** | **0.465** | **0.467** | **0.468** |
| 8 | ant-robot | **0.327** | **0.341** | **0.350** | **0.355** | **0.360** |
| **String in two way lane marked off with walls** | | | | | | |
| 9 | standard robots | **0.484** | **0.488** | **0.484** | **0.486** | **0.488** |
| 10 | standard robots sensors shifted | **0.463** | **0.468** | **0.466** | **0.465** | **0.464** |
| 11 | trail robots | **0.475** | **0.478** | **0.477** | **0.479** | **0.480** |
| 12 | trail robots sensors shifted | **0.463** | **0.465** | **0.464** | **0.464** | **0.464** |
| 13 | ant-robots | **0.347** | **0.370** | **0.382** | **0.388** | **0.395** |
| **String in open space** | | | | | | |
| 14 | standard robots | **0.477** | **0.480** | **0.480** | **0.480** | **0.481** |
| 15 | standard robots sensors shifted | **0.478** | **0.478** | **0.480** | **0.481** | **0.482** |
| 16 | trail robots | **0.461** | **0.465** | **0.466** | **0.465** | **0.465** |
| 17 | trail robots sensors shifted | **0.474** | **0.478** | **0.478** | **0.478** | **0.478** |
| 18 | ant-robots | **0.330** | **0.346** | **0.358** | **0.371** | **0.383** |

Table 1: Average speeds of strings at several clock ticks. Layouts of the highway are: rows 1 to 5 as in figure 9; rows 6-8 lay out as figure 10; rows 9-13 as in figure 13 and rows 14-18 as in figures 7 and 8

# 5 Swarm Traffic

The previous section dealt with simulations of traffic in prearranged string patterns. In this section we explore whether any patterns emerge naturally, or in other words whether and how the swarms themselves organize the traffic. Doing so we also have a look at how well the swarms perform using these patterns. The results obtained for string patterns (table 1) provide an upper-bound for the throughput or flow on the highway. Despite the expectation that lanes are less efficient than strings, lane patterns are better then unorganized traffic. As discussed above in we apply three types of robots: standard robots, trail robots and ant robots. For each type of robot we run simulations with swarms of various sizes. The swarms and the highway and trail are described in subsection 4.3 above.

## 5.1 Lanes in open space

We first explore the traffic of standard robots in open space. The swarms develop several lane patterns refer to the table 2. The swarm of 52 standard robots (row 1 of table 2) generates four lanes or one way zones as shown in figure 7. The swarm of 52 robots with shifted sensors develops two major lanes and three additional lanes are utilised by one and two robots only. The swarm of 42 robots with shifted sensors happens to create a six lane pattern with in the lanes from left to right 3, 2, 12, 13, 6 and 6 robots. The swarm of 26 maintains the initial four lanes with 7 and 6 robots which become equally spaced. The

| | *Average speed up to clock tick* / *Type of robot* | *150* | *300* | *600* | *1200* | 600-1200 | Number of lanes |
|---|---|---|---|---|---|---|---|
| | **Open space 52 robots** | | | | | | |
| 1 | standard robots | **0.417** | **0.449** | **0.463** | **0.471** | **0.479** | **4** |
| 2 | standard robots shifted sensors | **0.421** | **0.442** | **0.463** | **0.472** | **0.480** | **5(=2+3)** |
| | **Open space 42 robots** | | | | | | |
| 3 | standard robots | **0.419** | **0.448** | **0.463** | **0.471** | **0.480** | **4** |
| 4 | standard robots shifted sensors | **0.413** | **0.443** | **0.461** | **0.470** | **0.479** | **5** |
| | **Open space 37 robots** | | | | | | |
| 5 | standard robots | **0.429** | **0.456** | **0.466** | **0.473** | **0.480** | **4** |
| 6 | standard robots shifted sensors | **0.443** | **0.463** | **0.475** | **0.475** | **0.475** | **5** |
| | **Open space 26 robots** | | | | | | |
| 7 | standard robots | **0.467** | **0.474** | **0.477** | **0.479** | **0.480** | **4** |
| 8 | standard robots shifted sensors | **0.469** | **0.475** | **0.477** | **0.479** | **0.480** | **4** |
| | **Open space 26' robots** | | | | | | |
| 9 | standard robots | **0.457** | **0.470** | **0.475** | **0.478** | **0.480** | **4** |
| 10 | standard robots shifted sensors | **0.469** | **0.475** | **0.477** | **0.479** | **0.480** | **4** |
| | **Open space 22 robots** | | | | | | |
| 11 | standard robots | **0.447** | **0.465** | **0.470** | **0.475** | **0.480** | **4** |
| 12 | standard robots shifted sensors | **0.442** | **0.463** | **0.469** | **0.475** | **0.480** | **4** |

Table 2: Lane development by standard robots in open space.

swarm of $26'$ develops two main lanes of 11 robots and two additional lanes of 2 robots only. As the table shows, the size of the swarm is not a good predictor for the number of traffic lanes. However, true for all sizes of standard robot swarms is that since they are not bound to a trail the lanes gradually spread out, the spacing between the lanes may become as wide as the range of the sensors. Overall we can concluded that in open space the swarms of standard robots generate quite stable lane patterns comprising four to six lanes. In the long run the spacing between these lanes becomes as wide as the range of the sensors on the robots' sides. We note that standard robots will not surpass this boundary; however robots with perfect sensors would continue to disperse over the plane (corollary 2.3). Note though that while in table 2 the speed is nearly the same for all swarms, it is slightly below the speed in strings, refer to table 1 rows 14 and 15.

### 5.1.1 Trails

The trail robots and the robot-ants are defined to follow a trail. The width of the trail has considerable impact on the number of lanes that will evolve. On a very narrow trail of width 3 *units* - that is twice the safety zone - a single robot blocks the thoroughfare, while on slightly wider trails an abundance of conflicts will occur. On a trail of width 10 *units* two robots can pass easily. Table 3 gives an overview of the results of various simulations with different trail widths, refer to section 4.3 for the table's conventions.

The trail width influences the number of traffic lanes in that on a wider trail more lanes may develop. However, as a comparison of the swarm sizes shows, with increased traffic density on the narrow trails the number of lanes generally reduces. The last column of table 3 gives the average speed of the robots in the simulation of the 52 swarms, the speed clearly increases with the trail width. The highest speed is reached by the trail following robots with shifted sensors, refer to rows $12-14$. The initial situations for the 26, the $26'$ and the 52 swarms are defined to be symmetric in $x$ and $y$ they produce often an even number of lanes. The initial situation of the 26 swarm (refer to figure 8 right) comprises of four lanes (width 10 *units*) and the pattern persists on the wider trails. The

| Swarm size<br>Type of robot | | 22 | 26 | 26' | 37 | 42 | 52 | 52 robots |
|---|---|---|---|---|---|---|---|---|
| | Trail robots | | | | | | | average speed |
| 1 | trail width 10 | **2** | **2** | **2** | **ns** | **2** | **2** | 0.379 |
| 2 | trail width 14 | **2** | **ns** | **2** | **2** | **2** | **2** | 0.414 |
| 3 | trail width 16 | **3** | **4** | **2** | **ns** | **2** | **ns** | 0.374 |
| 4 | trail width 18 | **3** | **4** | **2** | **3** | **2** | **3 ns** | 0.422 |
| 5 | trail width 20 | **3** | **4** | **ns** | **4** | **2** | **3** | 0.425 |
| 6 | trail width 24 | **ns** | **4** | **4** | **4** | **4 ns** | **2ns** | 0.421 |
| 7 | trail width 30 | **4** | **4** | **4** | **4** | **4 ns** | **4** | 0.450 |
| | Trail robots sensors shifted | | | | | | | |
| 8 | trail width 10 | **2** | **2** | **2** | **ns** | **2** | **2 ns** | 0.332 |
| 9 | trail width 14 | **3** | **4** | **2** | **2** | **2** | **2** | 0.431 |
| 10 | trail width 16 | **3** | **4** | **2** | **ns** | **ns** | **2 ns** | 0.379 |
| 11 | trail width 18 | **5 ns** | **4** | **3 ns** | **3** | **3** | **3** | 0.415 |
| 12 | trail width 20 | **4** | **4** | **4** | **3** | **3** | **2** | 0.458 |
| 13 | trail width 24 | **5 ns** | **4** | **4** | **4** | **3 ns** | **4** | 0.461 |
| 14 | trail width 30 | **5** | **4** | **4** | **4** | **3** | **4** | 0.466 |
| | Ant-robots | | | | | | | |
| 15 | trail width 10 | **2** | **4** | **2** | **ns** | **2** | **jam** | 0.130 |
| 16 | trail width 14 | **5** | **4** | **2** | **3** | **2 ns** | **2 ns** | 0.299 |
| 17 | trail width 16 | **5** | **4** | **2** | **3** | **4** | **3** | 0.385 |
| 18 | trail width 18 | **5** | **4** | **2** | **3** | **4** | **3 ns** | 0.374 |
| 19 | trail width 20 | **5** | **4** | **2** | **3** | **4** | **3 ns** | 0.392 |
| 20 | trail width 24 | **5** | **4** | **2** | **3** | **4** | **4** | 0.418 |
| 21 | trail width 30 | **5** | **4** | **2** | **3** | **4** | **4** | 0.424 |

Table 3: Lane development on a trail at clock tick 1200; *ns*: not stable; in the last column the average speed up to clock tick 1200

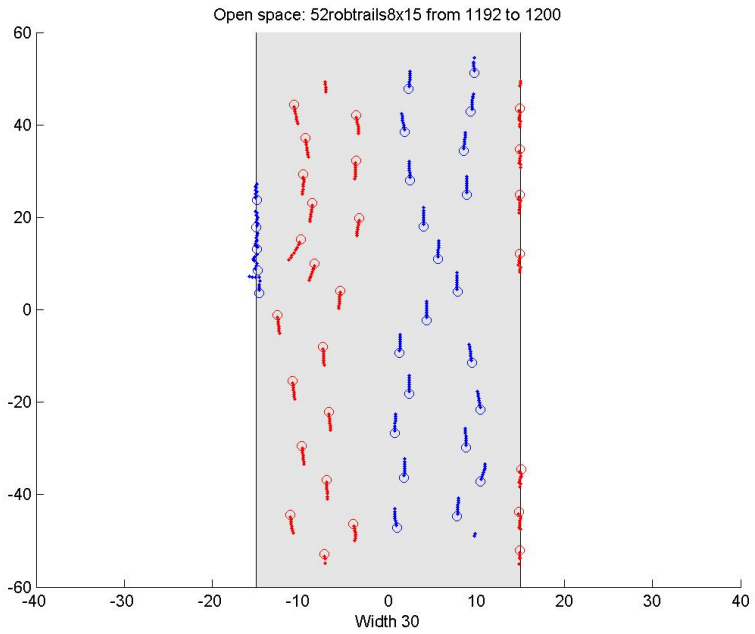


Figure 11: Swarm of 52 trail-robots on a trail 30 wide. Simulation results in table 3, row 7, column '52'.

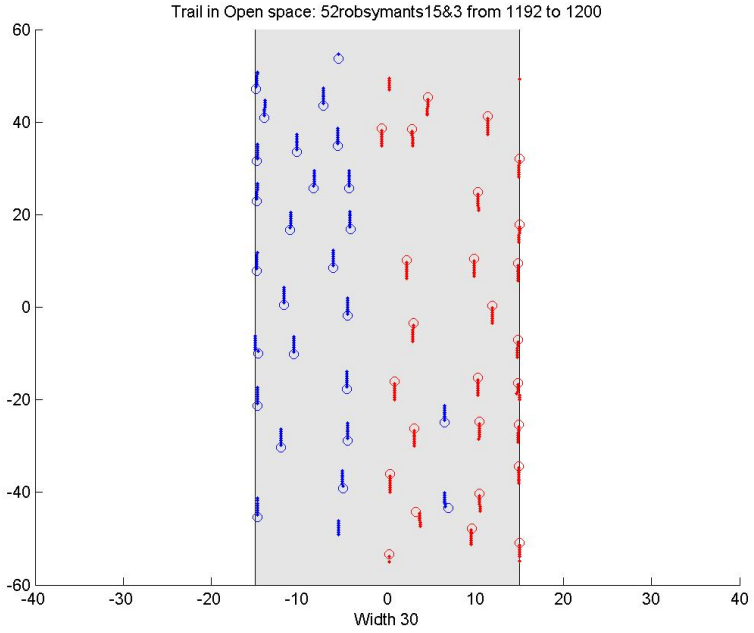


Figure 12: Swarm of 52 ant robots on a trail 30 wide. Simulation results in table 3, row 21, column '52'.

22 and 37 swarms are asymmetric and often produce odd numbers of lanes.

Figure 11 shows a four lane traffic pattern of trail robots on a trail 30 *units* wide and figure 12 shows the four lane traffic pattern of ant robots also with trail width of 30 *units*. The trail robots retain more distance between the lanes than the ant robots do. The explanation is that the trail robots' sensors range further sideways to a distance of 15 *units*, while the ants' sensors span only 10.60 *units* at the widest. Note also that whereas the trail robots generate curved lanes the ants travel in straight lines, again as is to be expected from their particular sensor system.

Overall we can concluded that in trails the swarms of robots generate quite diverse lane patterns varying form two to five lanes. In some cases no stable patterns have been observed. The trail robots and the ant robots are confined by the width of the trail and obviously the higher numbers of lanes occur in the wider trails. The spacing between the lanes varies with the sensor systems applied, the trail robots retain a wider spacing than the ant robots.

## 5.2 Lanes in bounded space

Above we have discussed lane development in open space. In this section we discuss simulations in a bounded space. We have two aims, the first is to produce a better comparison between standard robots and the trail and ant robots. The second aim is to study the effects of increasing the density of the swarm.

We fix the traffic area using two walls; the same structure we have used for the string simulations refer to section 4.3. The walls are visible only within a

| Swarm size | 26 | 26 | 26' | 26' | 37 | 37 | 42 | 42 | 52 | 52 |
|---|---|---|---|---|---|---|---|---|---|---|
| Type of robot | lanes | speed | lanes | speed | lanes | speed | lanes | speed | lanes | speed |
| standard robots | 2 | 0.420 | 2 | 0.464 | 2 | 0.327 | 2 at 2400 | 0.272 | jam | 0.154 |
| standard robots sensors shifted | 2 | 0.395 | 2 | 0.443 | 2 | 0.360 | 2 at 1800 | 0.275 | jam | 0.126 |
| trail robots | 2 | 0.398 | 2 | 0.448 | ns | 0.290 | 2 | 0.299 | jam | 0.117 |
| trail robots sensor shifted | 2 | 0.440 | 2 | 0.454 | 2 | 0.338 | 2 | 0.381 | jam | 0.191 |
| ant-robots | 2 at 1800 | 0.399 | 2 | 0.426 | jam | 0.248 | jam | 0.109 | jam | 0.059 |

Table 4: Swarm simulations in a walled space, 16 wide. Refer to figure 13 for layout

distances of 3 *units*; thus the 'free' space for the robots is effectively 10 *units*, which is also the trail width for the trail robots and the ant robots. Effectively, we force the standard robots to behave as if on a trail. As table 3 shows, on a trail of width 10 *units* the ant and trail robot swarms generate only two lanes; similarly the standard robot also generate only two lanes, refer to figure 13.

Table 4 shows the resulting average speeds in the simulation for swarms of sizes 22, 26, 37, 42 and 52. From left to right the traffic densities increase but the throughput goes down. For the 26 and 37 swarms the table shows average speeds up to clock tick 600. The larger swarms require more time to settle into a pattern, speed averages for the 42 and 52 swarms are given up to clock tick 1200.

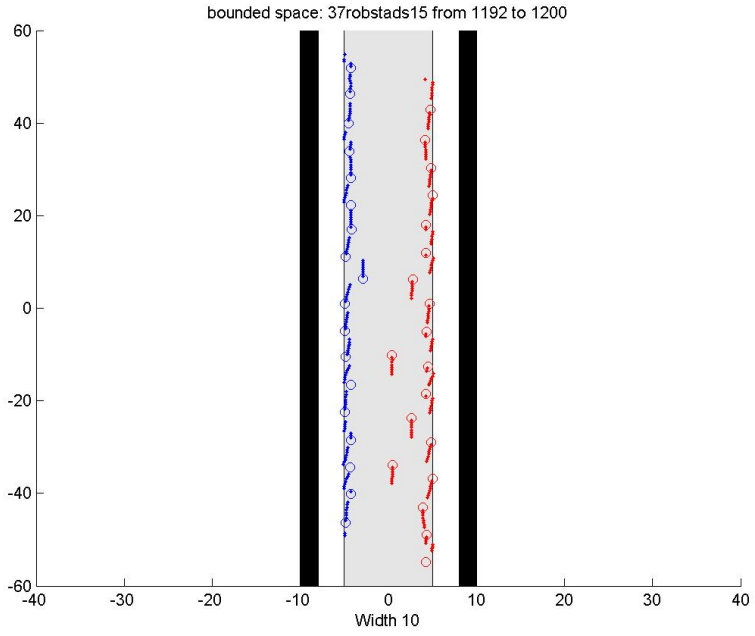


Figure 13: 37 Standard robots on a walled space 16 wide. Simulation results in table 4, row 1, column '37'.

The two types of standard robots perform the best at the lower densities due to their stronger tendency to seek wide spacing between the lanes, thus avoiding

head-on confrontations. We have seen before that they are also faster in strings. Nevertheless, with increasing density the average speed drops to half the value with the swarms of 42 and goes further down for the swarms of 52 robots. The trail robots with shifted sensors seem to cope best with increasing density, the swarm of 42 performs reasonably well; the ant robots are the poorest performers when traffic density increases. True for all types of swarms is that the swarms of 52 robots are too dense for the bounded space defined in the simulations. All 52 swarms start as expected at a low speed, but while the simulations continue the swarms remains entangled in a huge jam in which the swarms moves only very slowly, refer to figure 14 for an example. The jams didn't dissolve when doubling the simulation time.

Table 4 also shows that the number of robots present in a simulation is not a sufficient indicator for overcrowding; overcrowding is also dependent on the type of robots applied. In this sense our robot simulations confirm the findings in research on motorway traffic that road capacity and traffic flow are empirical variables; for road traffic study refer to (Maerivoet, 2006) for an overview or the USA, Highway Capacity Manual 2010 (Transportation Research Board, 2010) for regulations and definitions.

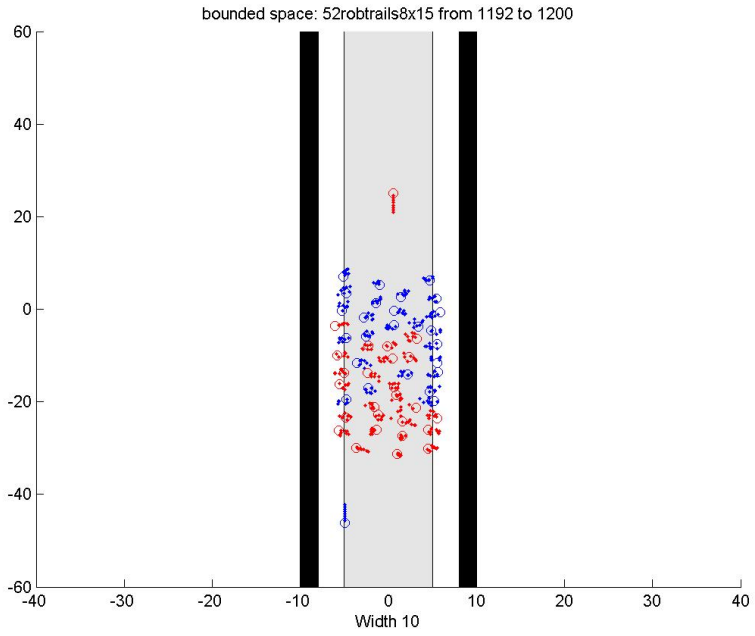


Figure 14: 52 Standard robots on a walled space 16 wide, in an unsolved jam. Simulation results in table 4, row 1, column '52'.

It is interesting to compare the trail robots in rows 1 and 8 of table 3 with table 4 rows 3 and 4. The swarms perform reasonably well in table 3, though the average speed is not very high stable two lane traffic patterns generate. While the 52 robot swarms in table 4 all remain stuck in a jam. The difference in the simulations for the trail robots is that in the latter simulations they are bounded

by a wall, a hard boundary which they cannot cross. In the simulations of table 3 the boundary of the trail is 'soft': the trail robots can cross it. The robots crossing the boundaries do not directly contribute to a high throughput of the swarm, but their stepping aside does contribute to the development of a traffic pattern and to traffic stability in the long run.

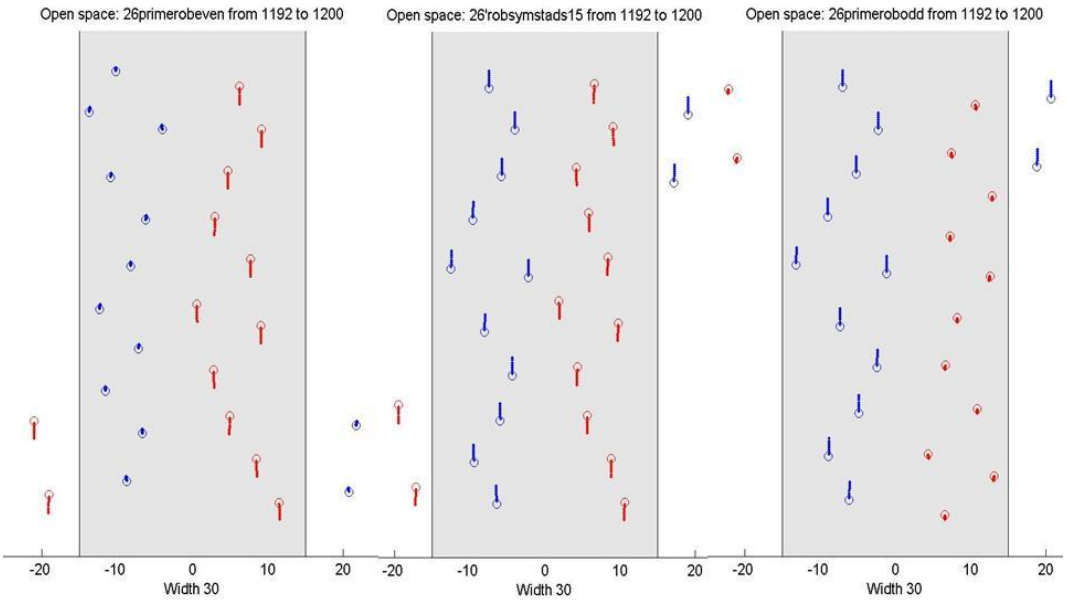


Figure 15: 26 Standard robots in open space, in the middle the simulation reported in table 2 row 9; left, the southbound group has the attraction reduced to 0.125; right, the northbound group has the attraction reduced to 0.125; the trail (30 wide) is drawn for reference only.

## 5.3 Qualitative differences

Above we have discussed simulations with swarms consisting of two groups. The difference between the groups consisted only of the traveling direction, either northbound or southbound. In all other respects the swarms were homogeneous. the swarms created traffic lane patterns of two to six lanes. Couzin and Franks (Couzin and Franks, 2003) reported on the triple lane pattern in army ants and their simulations of triple lanes. Our model creates the conditions in which triple lanes happen to occur. However, as the tables in this section show, the triple lane pattern is just one of several that do emerge. The latter observation means that we have not captured the essential condition that forces a swarm into a triple lane pattern.

Couzin and Franks (Couzin and Franks, 2003)(p.5), note that the throughput or flow of ants in their simulation is '*maximised when* $\omega = 1$ *(i.e. ants equally balance local conditions with their directional preference)*'. In our simulations above we have applied $\overrightarrow{EA}_{(G,a)} = 0.5 \times maxspeed = 0.5$. The attraction equals the repulsion generated by another robot at a distance of $(\sqrt{2} + 1.5) < 3$, refer

to equation (8). For comparison we made simulations of the 26′ swarm with the attraction reduced to a quarter: $\overrightarrow{EA}_{(G,a)} = 0.25 \times 0.5$ and simulations with the attraction doubled $\overrightarrow{EA}_{(G,a)} = 2{\times}0.5$. The 26′ ant robots developed the same two lane patterns, in all cases with normal, reduced and doubled attraction applied, the major difference observed is that when the attraction is less dominant the swarms claim wider lanes. Thus, though the throughput or flows differ, the lane patterns are similar.

In (Couzin and Franks, 2003)(p.5) it is further observed that there is a 'qualitative difference' between inbound and outbound ants, the outbound ants *'exhibit a higher rate of turning during avoidance manoeuvres'*. To model this difference between the two groups, we applied double and reduced attraction of the goal for one group only. Thus for one group the goal becomes (relatively) more dominant or in other words reducing the (relative) willingness to turn in the presence of other robots. In the standard setting with $\overrightarrow{EA}_{(G,a)} = 0.5$ the 26′ standard robot swarm developed a four lane pattern, with from left to right 2, 11, 11 and 2 robots (refer to figure 15 middle). Simulations with $\overrightarrow{EA}_{(G,a)} = 0.125$ for one group are shown in figure 15 on the left and right hand sides. We note that in figure 15 left and right the lanes and positions of the groups applying 0.5 attraction are nearly copies of the respective patterns in the standard simulation shown in the middle, while the simulation has been running as long as 1200 clock ticks. The groups with reduced attraction have claimed slightly wider lanes. Simulations with a swarm of $52 = 26 + 26$ ants and attraction for one group reduced other conditions the same as the simulations in table 3 produced the following results. On a trail of 10 *units* wide the swarm remained stuck in a jam; three lanes emerged on a trail of 14 *units* and four lanes on the trails of 16 *units* and 20 *units* wide. As with all simulations, once lane patterns have developed they endure, differences in turning rate do not matter in that respect. From the variety of patterns generated, we conclude that the difference in turning rate between the two groups is also not the essential condition for generating a three lane pattern. For a three lane pattern to emerge from a situation where the groups are well mixed, one group must have an inclination to 'seek' for the middle ground. A difference in turning rate does not induce a preference for the middle.

# 6 Conclusion

We explored with deterministic simulations when and under what conditions traffic lanes occur in the robot swarm traffic. Lane patterns occur frequently, however depending on the available space, trail width and range of the sensors the number of lanes varies from two to six. The mathematical intuition that if no head-on encounters occur existing lane pattern will be preserved are confirmed in our simulations. Once lanes have emerged, the lane patterns are stable and robust.

Overall, the standard robots are, due to their full sensor system, the most efficient and on the long run the spacing between the lanes becomes as wide as the range of the sensors on the robots' sides. Below a certain traffic density lane patterns emerge with all types of robots and ants, however dense swarms show some congestion and instability; extreme overcrowding keeps all swarms

entangled in huge jams.

In our model the triple lane pattern reported in (Couzin and Franks, 2003), is just one of the patterns occurring in the swarm traffic. Their assumption that a difference in turning rate does induce a preference for the middle ground does not hold in our simulation. This seems to indicate that either the particular initial situation or additional parameters -overlooked by ourselves and Couzin and Franks (2003)- force army ants into a triple lane pattern.

We have made simulations with trails, where the robots may cross boundaries, and highways with hard boundaries which cannot be crossed. While the boundary crossing robots do not directly contribute to a high throughput of the swarm, their stepping aside does contribute to the development of traffic lanes and traffic stability in the long run.

Our original question was whether we should organize the robot traffic explicitly or whether a certain regularity develops 'naturally'. Our (simplified) theoretical model has shown that lane patterns will not be disturbed. The simulations show that a variety of lane patterns may occur and once a pattern has emerged it is stable. The development of the lane patterns depends strongly on the initial situation, thus to organise our swarm traffic (and obtain a good throughput) it suffices to 'seed' a lane pattern, for instance by regulating how robots enter the high way; the swarm autonomously maintains the pattern.

Traffic density can considerably delay or even prevent the emergence of lanes. The remaining open problem is to define traffic density and to pin point overcrowding in order to predict congestion. Though the number of robots per $unit^2$ is an indicator, the simulations with different robots and ant robots show that also the type and range of the sensor system has to be taken into account.

The lane patterns reported in this paper emerged and endured on a straight stretch of highway. Future research will focus on situations where traffic junctions occur; at junctions the lane patterns are inevitably disturbed by crossing robots.

## Ackowledgement

The authors wish to acknowledge partial financial support from the European Union through the GUARDIANS project (IST-045269).

## References

L. Alboul, J. Saez-Pons, and J. Penders. Mixed human-robot team navigation in the guardians project. In *International Workshop on Safety Security and Rescue Robotics (SSRR 2008)*, 2008.

J. C. Baez and N. R. Gilliam. An algebraic approach to discrete mechanics. *Lett. Math. Phys.*, 31:205–212, 1994.

G. Baldassare, S. Nolfi, and D. Parisi. Evolving mobile robots able to display collective behaviour. In C. Hemerlijk, editor, *International Workshop on Self-Organisation and Evolution of Social Behaviour*, pages 11–22. Zurich:ETH, 2002.

G. Beni. From swarm intelligence to swarm robotics. In *Swarm Robotics: SAB 2004 International Workshop, Santa Monica, CA, USA, July 17, 2004, Revised Selected Papers*, pages 1–9. Lecture Notes in Computer Science, Springer Verlag, 2005.

D.J.T. Buhl, J.and Sumpter, J. Couzin, I.D.and Hale, E. Despland, E. Miller, and S.J. Simpson. From disorder to order in marching locusts. *Science*, 312: 1402–1406, 2006.

I. D. Couzin and N. R. Franks. Self-organised lane formation and optimized traffic flow in army ants. *Proc. R. Soc. Lond.*, B 270(2):139–146, 2003.

V. Crespi, A. Galstyan, and K. Lerman. Top-down vs bottum-up methodologies in multi-agent system design. *Autonomous Robots*, 24(3):303–313, 2008.

S. Darbha and Rajagopal K.R. Intelligent cruise control systems and traffic flow stability. *Transportation Research Part C*, 7:329–352, 1999.

M. Dorigo and T. Stutzle. *Ant Colony Optimization*. MIT Press, 2004.

P. Flocchini, G. Prencipe, N. Santoro, and P. Widmayer. Gathering of asynchronous robots with limited visibility. *Theoretical Computer Science*, 337: 147–168, 2005.

V. Gazi. Swarm aggregations using artificial potentials and sliding mode control. *IEEE Transactions on Robotics*, 21(6):1208–1214, 2005.

V. Gazi and K.M. Passino. Stability analysis of social foraging swarms. *IEEE Transactions on Systems, Man and Cybernetics-Part B: Cybernetics*, 34(1): 539–557, 2004a.

V. Gazi and K.M. Passino. A class of attraction/repulsion functions for stable swarm aggregations. *Int. J. Control*, 77(18):1567–1579, 2004b.

D. Helbing, P. Molnar, I. Frakas, and K. Bolay. Self-organising pedestrian movement. *Environment and Planning B: Planning and Design*, 28:361–383, 2001.

S Kazadi. Model independence in swarm robotics. *International Journal of Intelligent Computing and Cybernetics*, 2(4):672–694, 2009.

S. Kazadi, M. Ching, B. Lee, and R. Cho. On the dynamics of clustering systems. *Robotics and Autonomous Systems*, 46(2):1–27, 2003.

O. Khatib. Real-time obstacle avoidance for manipulators and mobile robots. *Int. J. Robotics Research*, 5(1):90–98, 1986.

B. Krogh. A generalized potential field approach to obstacle avoidance control. In *SME conf. Proc. Robotics Research: The next five years and beyond*, pages 11–22, 1984.

M. Latombe. *Robot motion planning*. Kluwer Academic Press, 1991.

L.-F. Lee. Decentralized Motion Planning within an Artificial Potential Framework (APF) for Cooperative Payload Transport by Multi-Robot Collectives. Master's thesis, State University of New York at Buffalo, 2004.

S. Maerivoet. *Modelling Traffic on Motorways: State-of-the-Art, Numerical Data Analysis, and Dynamic Traffic Assignment.* PhD thesis, Katholieke Universiteit Leuven, June 2006.

J.K. Parrish and W.M. Hamner, editors. *Animal groups in three dimensions.* Cambridge University Press, 1997.

J. Penders, L. Alboul, U. Witkowski, A. Naghsh, J. Saez-Pons, S. Herrechtsmeier, and M. El-Habbal. A robot swarm assisting a human fire-fighter. *Advanced Robotics*, 25:93–117, 2011.

J.S.J.H. Penders, L.S. Alboul, and Braspenning P.J. The interaction of congenial autonomous robots: Obstacle avoidance using artificial potential fields. In *Proceeding ECAI-94*, pages 694–698. John Wiley and Sons, 1994.

J.S.J.H. Penders, L. Alboul, and M. Rodrigues. Modelling interaction patterns and group behaviour in a three-robot team. In *Towards Autonomous Robotoc Systems, TAROS 04*, pages 1372–1382. University of Essex, 2004. ISSN 1744-8050.

J. H. Reif and H. Wang. Social potential fields: A distributed behavioral control for autonomous robots. *Robotics and Autonomous Systems*, 27(3):171–195, May 1999.

Transportation Research Board, editor. *Highway Capacity Manual 2010 (HCM2010)*, volume 1-4. Transportation Research Board. 500 Fifth St. NW, Washington, D.C., 2010. ISBN 978-0-309-16077-3.

T. Vicsek, A. Czirk, E. Ben-Jacob, and I. Cohen. Novel type of phase transition in a system of self-driven particles. *Physical Review Letters*, 75(6):1226–1229, 1995.

S.B. Young. Evaluation of pedestrian walking speeds in airport terminals. *Transportation Research Record*, (1674):20–26, 1999.